World Journal of Nanoscience and Nanotechnology

Research Article

Cerium-Based Coordination Polymer Sub-microspheres: Rapid Microwave Synthesis and their Thermal Conversion to Multi-Yolk-Shell CeO_2 Hollow Spheres

*Caiyun Dong, Yuanyuan Liao, Yuan Li and Shengliang Zhong**

College of Chemistry and Chemical Engineering, Jiangxi Normal University, China

Abstract

In this work, Cerium-based Coordination Polymer (CeCP) sub-microspheres were synthesized by using pyridine-2, 5-dicarboxylic acid as ligand *via* a facile microwave heating method. Multi-yolk-shell CeO_2 spheres with diameter of ranging from 300 nm to 500 nm were successfully prepared by calcination of the CeCP sub-microspheres. The as-synthesized products were characterized by SEM, FT-IR, XRD, TG, etc. Results show that the band gap (Eg) of the multi-yolk-shell CeO_2 is 2.79 eV. In addition, the photocatalytic properties of the obtained products were investigated. It is a nice catalyst for Rhodamine B (RhB) degradation under visible-light irradiation.

Keywords: Yolk-shell; Rare earth; Coordination polymer; CeO_2; Microwave

Introduction

Among rare earth compounds, rare earth oxides (RE_2O_3) have unique structure and physical and chemical properties, which have attracted a large number of researchers. RE_2O_3 has become the most important commercial rare earth compounds because of their broad applications. CeO_2, as one of the most active rare earth metal oxide, has been under extensive investigation for its several key applications in catalysts, fuel cells, sensors, UV blocking and luminescence [1-5]. It demonstrates the excellent activity of CeO_2 in many catalytic reactions mainly due to its abundant oxygen vacancy defects, high oxygen storage capacity and ability to relatively readily shuttlecock between III and IV oxidation states [6,7]. Therefore, the preparation and application of ceria have drawn more and more attention.

To date, CeO_2 with different shapes and structure have been successfully prepared by various methods [5,8]. In the past years, our group has also devote some effort to the preparation of ceria and ceria with different morphologies such as hierarchical architectures [9], microflowers [10], microdisks [11], nanoparticles [12], microspheres [13] and nanobelts [14] were obtained from the polymeric precursor method.

Materials with multi-yolk-shell architecture are of particular interest because of their special structure [15,16]. Chen et al. [17] has rationally designed and synthesized a novel CuO@C multi-yolk-shell octahedra composite structure *via* a simple solvothermal method and a two-step annealing process. Qi et al. [18] has reported a general self-templating method to achieve triple-shelled CeO_2 hollow microspheres, which are composed of tiny CeO_2 nanoparticles. Recently, we have successfully prepared multi-yolk-shell ceria hollow spheres using a template-free route [19]. By finely controlling the reaction parameters such as reaction time, molar ratio of reagent, and calcination temperature, ceria with tunable shell number and structures could be prepared. However, the methods mentioned above are still time and energy consuming.

Microwave-assisted reaction is carried out within a microwaves oven, ensuring a more homogeneous heating of the reagents mixture, the heat needed for the reaction is generated within the mixture, without the necessity of an external source [20]. And microwave allows rapidly obtaining considerable amounts of phases that are stable at high temperature (oxides, nitrides, carbides) and characterized by nanometer size, high specific surface area and high defectivity, all parameters that are crucial for catalytic applications, as well [21]. As is well known, microwave-assisted reaction has demonstrated its powerful benefits for greatly reducing the experiment time and holding promise for potentially large-scale industrials production [22-24]. Based on the successful synthesis of CeO_2 with core-shell structure [19], the approach of synthesizing core-shell cerium oxide by microwave method was studied. The CP with cerium as the center was synthesized by using 2,5-pyridinedicarboxylic acid (2,5-H_2PDC) as the ligand, and the multi-yolk-shelled CeO_2 nanomaterials with good morphology were successfully prepared by calcination. The effect of reaction parameters on the structure and morphology of the

Citation: Dong C, Liao Y, Li Y, Zhong S. Cerium-Based Coordination Polymer Sub-microspheres: Rapid Microwave Synthesis and their Thermal Conversion to Multi-Yolk-Shell CeO_2 Hollow Spheres. World J Nanosci Nanotech. 2018; 1(1): 1001.

Publisher Name: MedText Publications LLC

Manuscript compiled: October 05th, 2018

***Corresponding author:** Shengliang Zhong, College of Chemistry and Chemical Engineering, Jiangxi Normal University, Nanchang, 330022, China, Tel: 86079188120386; Fax: 86079188120386;

E-mail: slzhong@jxnu.edu.cn

product was investigated. The results showed that the CeO_2 prepared by microwave method had stronger ability to absorb ultraviolet light than that of mixed solvent.

Experimental Sections

Synthesis of multi-yolk-shell CeO_2 hollow nanospheres

In a typical experiment, 0.1 mmol $Ce(NO_3)3.6H_2O$ was dissolved in 10 mL absolute ethanol and then 10 mL of N, N-dimethylformamide (DMF) solution dissolved with 0.3 mmol 2,5-pyridinedicarboxylic acid (2,5-H_2PDC) was added to the above solution under stirring. After the mixed solution was stirred for 20 min, it was placed in the microwave oven (MDS-6G) setup and heated at 180°C for 30 min. After cooling to room temperature, the collected CeCP was separated by centrifugation and washed three times with absolute ethanol and deionized water, and dried at 80°C in vacuum drying oven. Finally, multi-yolk-shelled CeO_2 hollow nanospheres were obtained by calcination of the CeCP in air at 600°C for 4 h with a heating and cooling rate of 1°C min^{-1} and light yellow products were obtained.

Results and Discussion

Characterization and structure of the CeCP precursor

Our strategy begins with the synthesis of CeCP particles by a microwave-assisted mixed-solvothermal route. From the SEM image of typical CeCP (Figure S1), we can see that the products consist of a large quantity of uniform nanospheres with an average diameter of 400 nm and each nanosphere has relatively smooth surface (Figure S1). The CeCP nanospheres are smaller than those prepared by traditional mixed-solvothermal method by us before, which have an average diameter of 500 nm [19]. Also, comparing the precursors prepared by self-templating method for multi-shelled CeO_2 hollow microspheres, the particles are with much smaller size [18]. The TEM images show that the inside of the nanospheres is entirely dark and demonstrates the precursor is composed of solid spheres (Figure 1). The EDS analysis of the precursor clearly reveals the presence of Ce, C, O and N (Figure S2). And the powder X-ray diffraction (PXRD) pattern for the precursor does not display the typical characteristic peaks (Figure S3), indicating that the Ce^{3+} in the CeCP is in a disordered coordination to the carboxylate groups. The precursor was subjected to thermal analysis in an air atmosphere to obtain the TG curve as shown in Figure S4. From room temperature to 600°C thermal decomposition process is roughly divided into two stages: the weight loss which is about 20% before 320°C corresponds to the weight of the physically absorbed water molecules and structured water molecule. The second stage in the range of 320°C to 500°C is about 40%, which can be attributed to the decomposition of pyridine-2,5-dicarboxylic acid [25]. In addition, the FT-IR spectra (Figure S5) exhibits a shift of C=O stretching frequency from 1,726 cm^{-1} to 1,586 cm^{-1}, demonstrating that carboxyl groups of the 2,5-H2PDC have coordinated with Ce^{3+} [26]. Based on the above analysis, a conclusion can be safely drawn that CeCP was formed.

Influence of different reaction parameters on the morphology of the CeCP precursor

Effect of metal-ligand ratio: In the process of studying the optimal reaction conditions for the preparation of the CeCP precursor, a series of exploratory experiments were conducted. When the reaction temperature and reaction time were fixed, the molar ratio of metal to ligand was varied; the obtained products were examined using SEM, as shown in Figure S6. When the molar ratio of metal to ligand is 1:1 and 1:2, some of the spheres are broken and many small spheres are not formed completely. Increasing the amount of ligand to 1:4, the majority of the spheres is broken and is not well dispersed. While the molar ratio was 1:3 (Figure S1), the spheres are well formed and uniform. Thereby, 1:3 was selected as the optimal molar ratio.

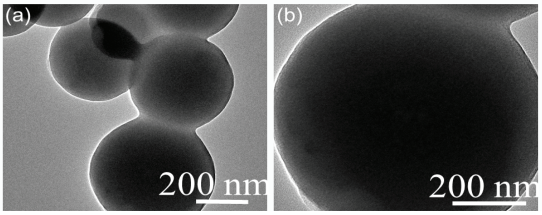

Figure 1: TEM images of the typical CeCP prepared microwave heating at 180°C for 30 min.

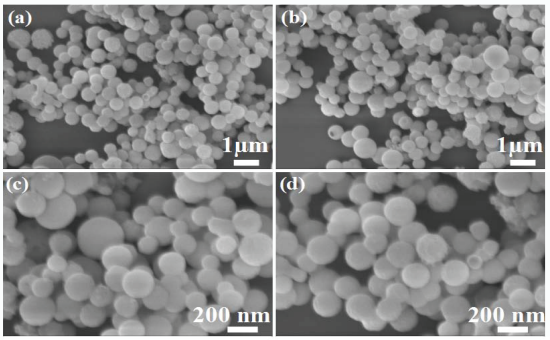

Figure 2: SEM images of as-prepared CeO2 prepared after thermal decomposition the typical CeCP in air at 600°C for 4 h.

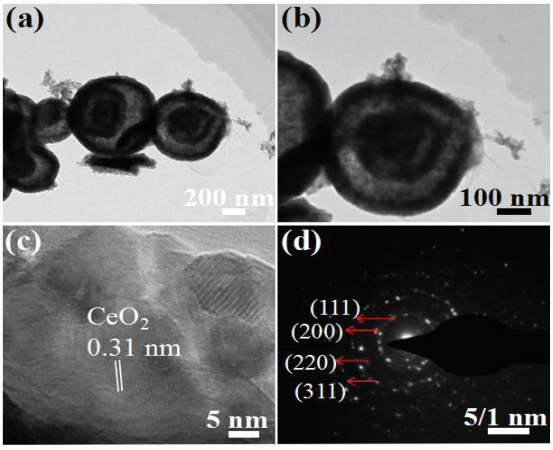

Figure 3: (a,b) TEM images; (c) HRTEM images and (d) SAED pattern of the product obtained after thermal decomposition of the typical CeCP sample in air at 600°C for 4 h.

Effect of the preparation temperature on the CP precursors: With other conditions unchanged, experiments were performed at different reaction temperature. When the temperature is below 140°C, nearly no product was obtained. So, 140°C, 160°C and 200°C were selected. Figure S7 shows the SEM images of different samples in this temperature gradient. At 140°C, the CeCP is composed of a large number of spheres. Compared to the typical CeCP products, these spheres are not very uniform in particle size and the particles are poorly dispersed. From the SEM images we can see that some

particles have not yet fully formed due to low reaction speed at low temperature. When the temperature was increased to 160°C, we can see a large number of balls generated, but the adhesion phenomenon is serious. However, the temperature reached 200°C, many spheres are broken and the spheres are not well formed.

Effect of the preparation time on the CP precursor: Finally, in order to study the formation of a typical product, a series of time-gradient samples were synthesized in the presence of reactant concentration and reaction temperature. Figure S8 is the SEM images of products prepared after different reaction times at 10, 20, 40 min, respectively. In the first 10 min of the reaction, we can see a small number of badly-formed spheres. When the reaction time was extended to 20 min, the products are still not well formed. Further prolonging the reaction time to 40 min, the product consisted of a large number of relatively uniform and dispersible pellets, which is similar with the product prepared after 30 min. Therefore, 30 min was selected as the optimal reaction time considering the energy saving and economic factors.

Morphology, crystalline phase and properties of multi-yolk-shell ceria

The typical sample was obtained after calcining the typical CeCP spheres at 600°C for 4 h in air to obtain the CeO_2 nanospheres. The SEM images in Figure 2 show that uniform CeO_2 nanospheres are in a large scale with an average diameter of 300 nm and a rough surface, such a morphological change can be attributed to the removal of the organic ligand meanwhile the gas is generated. Figure S9 presents the XRD pattern of the final calcined product. All the peaks could be indexed to the cubic ceria (JCPDS No. 34-0394), confirming the high purity of the final CeO_2. The EDX (Figure S10) of the precursor analysis confirms that the typical peaks corresponding to Ce and O elements and the atomic ratio of Ce/O is about 1:2. In order to explore the interior structure of these nanospheres, the CeO_2 nanospheres were further characterized by TEM and HRTEM. The TEM images shown in Figure 3a and 3b reveal that most nanospheres consist of several layers of shells and one relatively darker spherical core. The relatively darker spherical core is not solid but consisted of small hollow spheres. The HRTEM (Figure 3c) reveals the well-crystalline nature, well-resolved lattice fringes with inter-planar spacing of 0.31 nm and 0.19 nm are clearly visible, corresponding to the (111) and (220) atomic plane of the cubic phase ceria. The SAED ring patterns (Figure 3d) shows that the perfect multi-yolk-shelled hollow CeO_2 nanosphere is polycrystalline.

Properties of multi-yolk-shell ceria: As is well known, CeO_2 is an excellent UV absorption material. The UV-Vis absorption spectrum of the as-obtained CeO_2 is shown in Figure 4. The optical band gap Eg can be calculated based on the following equation: Eg=1,240/λAE, where λAE represents the edge wavelength of absorbance. The calculated CeO_2 absorption wavelength threshold is 443 nm, and the corresponding Eg is 2.79 eV, which is smaller than the commercial value of 2.82 eV. Compared with the core-shell ceria synthesized by solvothermal method (2.84 eV), the UV absorption capacity was improved. In general, the quantum size effect is the main reason for the increase in the forbidden band width [27]. The above results may therefore be that the nano-particles prepared by microwave-assisted heating are smaller in size, resulting in a red shift of UV-Vis [28].

The photodegradation of RhB was chosen to test the potential applicability of the as-synthesized CeO_2 as the recyclable photocatalyst by investigating their photocatalytic activity under UV light irradiation in aqueous solution. The suspension was stirred in the dark for 30 min to achieve the adsorption/desorption equilibrium among the catalyst and RhB molecules. The absorption peaks at 554 nm was observed for RhB and it confirms the photodegradation process [29]. The reaction process was recorded with time (t) in min under visible-light irradiation as shown in Figure 5. After each 20 min, 1.5 mL of UV reacted solution was taken and the absorbance changes of RhB were measured using UV-Vis spectrophotometer. It was clear that the light absorption peak of RhB is almost flat. After four-hour of UV light, we can observe the color changes of the dye solution from pink color to colorless. The result also indicated that the efficiency of dye decomposition achieved nearly 98%. To test the stability of CeO_2, the catalyst was collected by centrifugation and we examined for photodegradation of RhB during three cycle experiments under identical conditions (Figure 6). After three cycles, the photocatalytic activity of the CeO_2 remained almost unaffected. Finally, from the obtained results clearly indicate that the as-synthesized multi-yolk-shelled hollow CeO_2 nanosphere are with significant catalytic activity, hence this could be beneficial photocatalyst for the decomposition of color dye [30,31].

Conclusions

In summary, CeCP sub-microspheres were synthesized by microwave-assisted heating without the presence of template and any surfactant. The results show that the size and morphology of the CeCP can be controlled by changing the reaction parameters, such as reaction temperature, reaction time and molar ratio of metal to

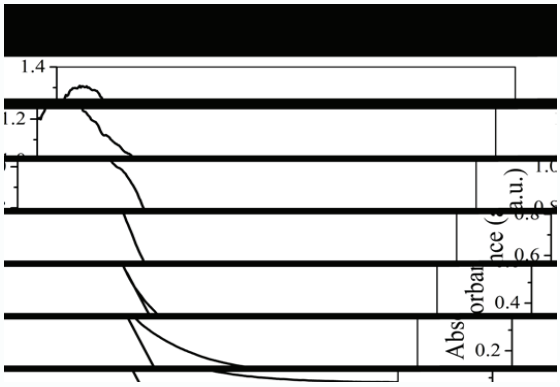

Figure 4: UV-Vis spectrum of the multi-yolk-shelled hollow CeO2 nanospheres.

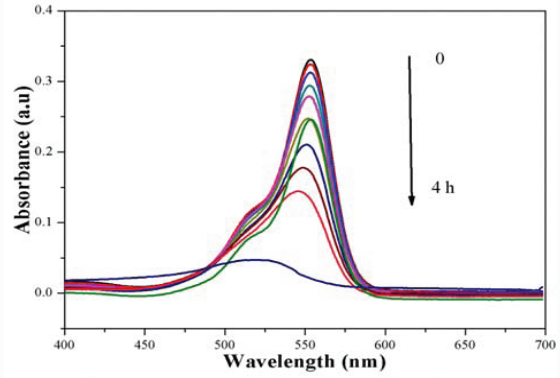

Figure 5: UV-Vis spectra for the catalytic reduction of the multi-yolk-shelled hollow CeO2 nanosphere as the catalysts at different time intervals.

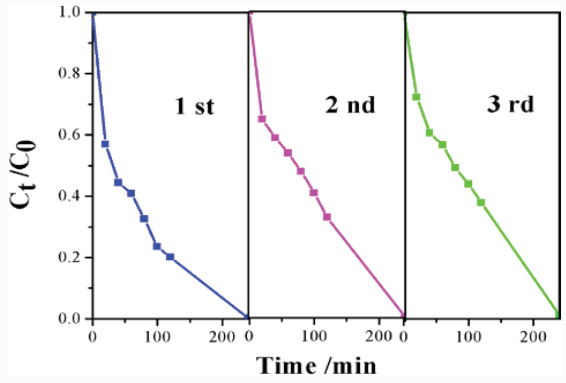

Figure 6: Recycling test of Ct/C0 ~t curves of photocatalytic degradation of RhB.

ligand. Multi-yolk-shelled hollow CeO_2 nanosphere can be obtained by calcining the precursor at air at 600°C for 4 h. In addition, compared with the UV absorption capacity of core-shell ceria synthesized by solvothermal and microwave methods, it was found that the core-shell ceria synthesized by microwave method exhibit much better UV absorption performance. As a photocatalyst, core-shell CeO_2 shows excellent degradation effect for RhB, which is nearly 98% under visible-light irradiation. This may be due to the formation of core-shell CeO_2 with more active surface area. It is hoped that more ongoing research efforts and simple way could be paid to the core-shell nanostructures.

Acknowledgement

This work was supported by the National Natural Science Foundation of China (Nos. 91622105), Jiangxi Provincial Department of Science and Technology (Nos. 20161BAB203083 and 20172BCB22008).

References

1. Cargnello M, Doan-Nguyen VV, Gordon TR, Diaz RE, Stach EA, Gorte RJ, et al. Control of metal nanocrystal size reveals metal-support interface role for ceria catalysts. Science. 2013;341(6147):771-3.
2. Graciani J, Mudiyanselage K, Xu F, Baber AE, Evans J, Senanayake SD, et al. Highly active copper-ceria and copper-ceria-titania catalysts for methanol synthesis from CO_2. Science. 2014;345(6196):546-50.
3. Park S, Vohs JM, Gorte RJ. Direct oxidation of hydrocarbons in a solid-oxide fuel cell. Nature. 2000;404(6775):265-7.
4. Walkey C, Das S, Seal S, Erichman J, Heckman K, Ghibelli L, et al. Catalytic properties and biomedical applications of cerium oxide nanoparticles. Environ Sci: Nano. 2015;2:33-53.
5. Sun C, Li H, Chen L. Nanostructured ceria-based materials: synthesis, properties, and applications. Energy Environ Sci. 2012;5:8475-505.
6. Campbell CT, Peden CH. Chemistry. Oxygen vacancies and catalysis on ceria surfaces. Science. 2005;309(5735):713-4.
7. Esch F, Fabris S, Zhou L, Montini T, Africh C, Fornasiero P, et al. Electron localization determines defect formation on ceria substrates. Science. 2005;309(5735):752-5.
8. Trovarelli A, Llorca J. Ceria catalysts at nanoscale: how do crystal shapes shape Catalysis?. ACS Catal. 2017;7(7):4716-35.
9. Wang L, Zhang LF, Zhong SL, Xu AW. Highly uniform CeO2 hierarchical microstructures: Facile synthesis and catalytic activity evaluation. Appl Surf Sci. 2012;263:769-76.
10. Zhong S, Wang M, Wang L, Li Y, Noh HM, Jeong JH. Preparation of 3D cerium-based coordination polymer microstructures and their conversion to ceria. CrystEng Comm. 2014;16:231-6.
11. Chen J, Zhong S, Liu Q, Wang Y, Wang S, Xu R, et al. Cerium sulfate microdisks prepared by a solvothermal method and their conversion to ceria microdisks. Powder Technology. 2010;197(1-2):136-9.
12. Wang L, Li Y, Zou H, Li X, Zhong S. Cerium-based coordination polymers micro/nanostructures: Room temperature synthesis and their thermolysis to ceria. Mater Manuf Process. 2017;32(5):484-8.
13. Nie ZW, Zeng CH, Xie G, Zhong SL. Uniform cerium-based coordination polymer microspheres: Preparation and upconversion emission. J Nanosci Nanotechnol. 2016;16(4):3705-9.
14. Li Y, Zou H, Qiao Z, Liao Y, Wang L, Zhong S. Fabrication of ultralong ceria nanobelts via a coordination polymer precursor method. New J Chem. 2018;42:3653-9.
15. Zhang Q, Lee I, Joo J, Zaera F, Yin Y. Core-shell nanostructured catalysts. Acc Chem Res. 2013;46(8):1816-24.
16. Li G, Tang Z. Noble metal nanoparticle@metal oxide core/yolk–shell nanostructures as catalysts: recent progress and perspective. Nanoscale. 2014;6(8):3995-4011.
17. Chen T, Hu Y, Cheng B, Chen R, Lv H, Ma L, et al. Multi-yolk-shell copper oxide@carbon octahedra as high-stability anodes for lithium-ion batteries. Nano Energy. 2016;20:305-14.
18. Qi J, Zhao K, Li G, Gao Y, Zhao H, Yu R, et al. Multi-shelled CeO2 hollow microspheres as superior photocatalysts for water oxidation. Nanoscale. 2014;6(8):4072-7.
19. Liao Y, Li Y, Wang L, Zhao Y, Ma D, Wang B, et al. Multi-shelled ceria hollow spheres with a tunable shell number thickness and their superior catalytic activity. Dalton Trans. 2017;46(5):634-44.
20. Ganesh I, Johnson R, Rao GVN, Mahajan YR, Madavendra SS, Reddy BM. Microwave-assisted combustion synthesis of nanocrystalline $MgAl_2O_4$ spinel powder. Ceram Int. 2005;31:67-74.
21. Tapas RS, Armandi M, Arletti R, Piumetti M, Bensaid S, Manzoli M, et al. Pure and Fe-doped CeO2 nanoparticles obtained by microwave assisted combustion synthesis: Physico-chemical properties ruling their catalytic activity towards CO oxidation and soot combustion. Appl Catal B: Environ. 2017;211:31-45.
22. Kappe CO. My twenty years in microwave chemistry: From kitchen ovens to microwaves that aren't microwaves. Chem Rec. 2018.
23. Baig B, Varma RS. Alternative energy input: mechanochemical, microwave and ultrasound-assisted organic synthesis. Chem Soc Rev. 2012;41(4):1559-84.
24. Zhu YJ, Chen F. Microwave-assisted preparation of inorganic nanostructures in liquid phase. Chem Rev. 2014;114(12):6462-555.
25. Li S, Zhang X, Hou Z, Cheng Z, Ma P, Lin J. Enhanced emission of ultra-small-sized LaF3:RE3+ (RE = Eu, Tb) nanoparticles through 1,2,4,5-benzenetetracarboxylic acid sensitization. Nanoscale. 2012;4(18):5619-26.
26. Isaeva Vera I, Belyaeva Elena V, Fitch Andrew N, Chernyshev Vladimir V, Klyamkin Semen N, Kustov Leonid M. Synthesis and structural characterization of a series of novel Zn(II)-based MOFs with pyridine-2,5-dicarboxylate linkers. Cryst Growth Des. 2013;13(12):5305-15.
27. Renuka NK. Structural characteristics of quantum-size ceria nano particles synthesized via simple ammonia precipitation. J Alloy Compd. 2012;513:230-5.
28. Yuan S, Zhang Q, Xu B, Jin Z, Zhang Y, Yang Y, et al. Porous cerium dioxide hollow spheres and their photocatalytic performance. RSC Adv. 2014;4(107):62255-61.

29. Maria Magdalane C, Kaviyarasu K, Judith Vijaya J, Siddhardha B, Jeyaraj B, Kennedy J, et al. Evaluation on the heterostructured CeO2/Y2O3 binary metal oxide nanocomposites for UV/Vis light induced photocatalytic degradation of Rhodamine-B dye for textile engineering application. J Alloy Compd. 2017;727:1324-37.

30. Ameen S, Akhtar Shaheer M, Kim Y, Yang OB, Shin HS. Synthesis and characterization of novel poly(1-naphthylamine)/zinc oxide nanocomposites: application in catalytic degradation of methylene blue dye. Colloid Polym Sci. 2010;288(16-17):1633-8.

31. King'ondu C, Opembe N, Genuino H, Garces H, Njagi E, Aparna I, et al. Nonthermal synthesis of three-dimensional metal oxide structures under continuous-flow conditions and their catalytic applications. J Phys Chem C. 2011;115(47):23273-82.